Interface formation in K doped poly(dialkoxy-p-phenylene vinylene) light-emitting diodes

H. H. P. Gommans[a] and A. W. Denier van der Gon
Department of Applied Physics, Eindhoven University of Technology, P.O. Box 513, 5600 MB Eindhoven, The Netherlands

G. G. Andersson
Wilhelm-Ostwald-Institut für Physikalische und Theoretische Chemie, Universität Leipzig, Linnéstrasse 2, 04103 Leipzig, Germany

L. J. van IJzendoorn, R. M. T. Pijper, and H. H. Brongersma
Department of Applied Physics, Eindhoven University of Technology, P.O. Box 513, 5600 MB Eindhoven, The Netherlands

(Received 16 May 2003; accepted 10 August 2003)

Manufacturing of Al/K/OC_1C_{10} poly(p-phenylene vinylene)/indium–tin–oxide light emitting diode structures by physical vapor deposition of K onto the emissive polymer layer has been characterized by electroluminescence and ion spectroscopy. Varying the deposited K areal density from 3.9×10^{12} to 1.2×10^{14} atoms cm^{-2} the external efficiency rises from 0.01 to 1.2 Cd A^{-1}. Spectra obtained by ion scattering analysis demonstrate the overall absence of K at the polymer outermost surface layer, and diffusion up to a depth of 200 Å. Depth profiles have been derived, and were modeled using an irreversible first order ''trapping'' reaction. Trapping may stem from confinement of the electron at a conjugated segment, that was donated through charge transfer typical for alkali/π-conjugated systems. This study demonstrates that evaporation of low work function metals onto organic systems should not be depicted as simple layered stacking structures. The enhanced electroluminescence with submonolayer K deposition is attributed to the shift of the recombination zone away from the Al cathode, which is demonstrated to prevail over the known exciton quenching mechanism due to the formation of gap states. © *2003 American Institute of Physics.*
[DOI: 10.1063/1.1614864]

I. INTRODUCTION

Conjugated organic materials have drawn much attention for their properties and technological potential in electronic devices. Since the discovery of electroluminescence (EL) in poly(p-phenylene vinylene) (PPV),[1] many investigations have focused on the development of efficient *p* light emitting diodes (LEDs). An important aspect in this is the analysis of metal/organic interfaces, which play a major role in the conduction, efficiency and stability of the device. Contributions in this field arose among others from ultraviolet photoelectron spectroscopy (UPS), which demonstrated the formation of gap states, (bi)polarons,[2–5] the failing of vacuum level alignment,[6,7] and energy level bending.[8] By photoluminescence (PL) experiments it was also shown that metal deposition resulted in exciton quenching by either directly introducing gap states[9] or opening a nonradiative decay channel through energy transfer to a metal mirror.[10,11] Recently we have shown that the amount of Ca diffusing into the polymer during cathode deposition influences the electroluminescence.[12]

In order to estimate interface effects on the device performance, an important issue is its width. In typical modelling studies interfaces are often neglected and abrupt junctions are assumed.[13,14] However, from thermodynamics it is predicted that metals evaporated onto soft condensed layers are able to diffuse to extensive depths, depending primarily on chemical reactivity and kinetics.[15] Experimental investigations are lacking, despite that one of the major improvements in performance has been achieved by the introduction of interfacial layers between the cathode and the conjugated polymers. Here distinction can be made between dopant layers[16,17] and insulating layers,[18–21] where in the latter case controversy still exists about its operating mechanism.

Doping by physical vapor deposition of alkali metals has been established by UPS.[2–5] The alkali metal acts as a strong reducing agent that donates its electrons to the conjugated π system, which in turn leads to the generation of the earlier mentioned (bi)polarons. These states in the previously forbidden electronic band gap may effectivily reduce the barrier height for electron injection. Taking into consideration that the efficiency in PPVs is restricted by an unbalanced charge transport as a result of the lower electron mobility compared to the hole mobility, alkalies are expected to enhance the device performance severely. In addition Cao *et al.*[16] demonstrated an enhanced device stability with increasing alkali cation size and suggested an increased diffusion barrier underlying this observation. Diffusion of K in both PPV and poly(2-methoxy-5-(2′-ethyl-hexyloxy)-1,4-phenylene vinylene) (MEH–PPV) has in fact been identified by angle-resolved x-ray photoelectron spectroscopy (XPS).[22] However

[a]Author to whom correspondence should be addressed; electronic mail: h.h.p.gommans@tue.nl

the XPS probe depth is confined to a range of 5–20 atomic layers with a maximum sensitivity of 1 at % and while qualitative information is readily available quantitave diffusion profiles were not extracted.

Although this brief overview points to a correlation between metal diffusion and conductivity and radiative recombination in PPVs, no direct evidence has been established. Also literature on alkali metals employed as electron injection electrode in LEDs[16,23] is rather limited. In this article we will focus on K deposited onto poly(dialkoxy-p-phenylene vinylene) $OC_1C_{10}PPV$[24] by physical vapor deposition. The interface formation is studied by inspection of the K distribution in $OC_1C_{10}PPV$ using ion scattering analysis techniques and diffusion profiles are extracted. The results are correlated to the LED performance derived from EL measurements.

II. EXPERIMENT

A. Sample preparation and electroluminescence

Indium–tin–oxide (ITO)-coated glass substrates were cleaned in ultrasonic baths of aceton and propanol for 30 min each. Subsequently they were introduced into the ultraviolet (UV)-ozone cleaning chamber, which is directly attached to a glovebox ($[O_2]<1$ ppm and $[H_2O]<1$ ppm).[25] After 30 min of UV-ozone treatment hydrocarbons were effectively removed from the substrates, the chamber was evacuated, refilled with nitrogen, and the substrates were transferred into the glovebox setup. An $OC_1C_{10}PPV$ 0.7 wt % toluene solution was heated at 50 °C for 1 h and dropcast at a spinrate of 3100 rpm. Typical film thicknesses were determined to be 120 ± 10 nm by an alpha-stepper (Alpha-step 200 Tencor Instruments). By means of a transfer chamber these samples were introduced into an ultrahigh vacuum (UHV) vapor deposition chamber (base pressure 10^{-9} mbar) without being exposed to air. The cathodes were deposited through a shadow mask that defined six diodes per substrate with an active area of 24 mm^2. K was deposited from an alkali metal dispenser purchased from Saesgetters (~800 °C; 2×10^{-9} mbar). For the LEDs an Al capping layer (~80 nm) was deposited by evaporation (~1 Å/s) while the thickness was monitored using a quartz crystal (1250 °C; 10^{-7} mbar). Directly after lowering the temperature of the Al effusion cell to 600 °C, EL measurements were conducted in an *in situ* setup in the evaporation chamber at a temperature of 36 °C. Several runs were repeatedly made with increasing evaporation time for K. In order to perform the ion scattering analysis the Al capping layer was omitted and samples were transported in an airtight suitcase to the ion scattering setups. In order to conduct the neutral impact collision ion scattering spectroscopy (NICISS) measurements, the samples had to be brought into contact with air for several minutes.

B. Ion scattering analysis

In order to study K diffusion into $OC_1C_{10}PPV$ two different ion scattering techniques have been employed, viz. low energy ion scattering (LEIS) and NICISS.

LEIS probes the elemental composition of the topmost atomic layer: the mass of the surface atoms is determined from analysis of the kinetic energy of elastically backscattered noble gas ions, while efficient neutralization of the ions ensures the surface sensitivity.[26] LEIS measurements were performed in an UHV system with a base pressure of 2×10^{-10} mbar. A monoenergetic 3 keV $^3He^+$ ion beam was employed and the applied ion dose was typically between 10^{13} and 10^{14} atoms/cm^2. In the setup, the kinetic energy of ions scattered by 145° was analyzed and detected by a double toroidal analyzer and position sensitive detector[27] and allowed for a detection limit of 100 ppm in the case of K.

By measuring the time of flight (TOF) of the charged plus neutralized noble gas ions, the composition in deeper layers can be studied with NICISS.[28,29] Passage through the material induces additional inelastic loses due to small-angle scattering and electronic excitation (nuclear and electronic stopping power). In order to obtain absolute concentration-depth profiles, the stopping power in hydrocarbons,[30] the detector sensitivity, and differential cross sections must be determined.[31] NICISS measurements were conducted in a high vacuum system with a base pressure of $\sim4\times10^{-6}$ mbar. A monoenergetic 4.5 keV $^4He^+$ ion beam was employed with a maximum dose of 5×10^{13} atom/cm^2. In this setup, the scattering angle is fixed to 168° with the analyzer detector orientation along the surface normal. The concentration sensitivity is also close to 100 ppm for K. The depth resolution is best near the surface and decreases slowly with depth ($\leqslant$10 Å at 100 Å depth).[31] By integration of a NICISS spectrum we obtain the total amount of deposited K up to a depth of 200 Å.

Ion scattering methods generally induce modifications in the chemical structure of polymer surfaces.[32] Hence in order to probe the intrinsic surface composition, a dose of $\sim10^{13}$ ions/cm^2 is required which allows for ''static'' conditions.[33] Although such a dose already damages the polymer, the spectra do not show any significant composition modification during the measurement. Surface charging appeared to be negligible for the applied film thickness due to the conducting property of PPV.

III. RESULTS

A. Electroluminescence

The luminance and current versus bias are shown in Figs. 1 and 2 for different amounts of deposited K. A dramatic increase of more than 2 orders of magnitude in light output with increasing K deposition is observed. The light onset shifts from 4.50 down to 1.85 V, the latter corresponding to the lowest conceivable onset potential for radiative emission of the polymer layer ($\lambda_{max}=630$ nm; see Fig. 3). Already at a deposition of 2.0×10^{13} atoms/cm^2 the current onset has shifted from 1.00 ± 0.05 to 1.25 ± 0.05 V, resulting in a reduced current at low bias, which converges to its original value with increasing bias. This effect will be explained by an increase in built-in potential in the subsequent discussion. The maximum efficiency increases from 0.01 to 1.2 Cd/A and saturates at higher amounts of deposition (Fig. 4). Moreover the bias at which this maximum is obtained decreases with K coverage to almost 2.0 V, which is close to the light onset. Obviously, the amount of K deposition dic-

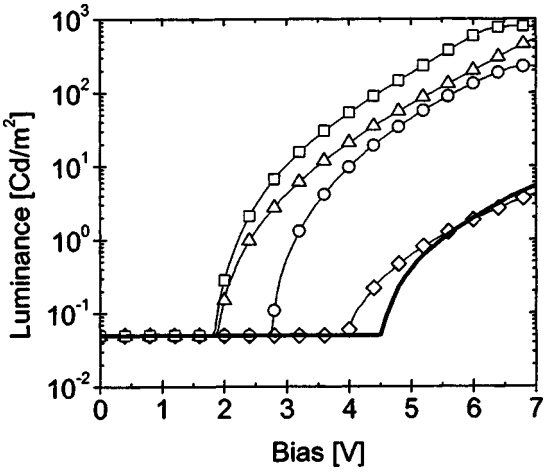

FIG. 1. EL vs bias on Al/K/OC_1C_{10}PPV/ITO stacking structures with varying deposition coverage: 3.9×10^{12} (diamonds), 2.0×10^{13} (circles), 3.4×10^{13} (triangles), and 1.0×10^{14} K (squares) atoms/cm^2 and without K (thick solid curve).

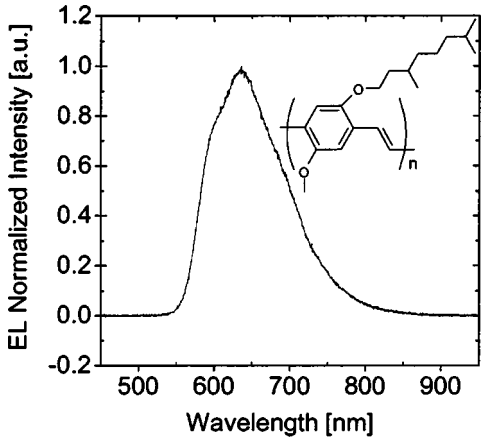

FIG. 3. EL spectrum normalized to its peak height for 1.0×10^{14} K atoms/cm^2. Inset gives the chemical structure of OC_1C_{10}PPV.

tates the device performance and hence, this regime is relevant in order to study the associated depth profiles.

B. Ion scattering spectroscopy

Figure 5 shows two LEIS spectra of OC_1C_{10}PPV/ITO substrates with different amounts of K deposition. The C and O surface peaks are the main features in the spectrum. The absence of a peak at 2265 eV, indicated by the arrow in the figure, shows that K completely diffuses into the polymer. We also observe a continuous background starting at 2265 eV due to reionization of the neutral atoms which were scattered in deeper layers. The extent of this signal indicates K diffusion up to at least 100 Å, but possibly much deeper. The increasing background at ion energies below 1000 eV originates from detection of ionized hydrogen recoils. In order to compare the C and O signals for different K coverages a LEIS spectrum with pristine OC_1C_{10}PPV is shown in the inset. After a correction for the increased background due to the diffusion of K, both surface peaks remain similar, confirming the absence of K at the outermost surface layer.

Figure 6 shows two NICISS spectra: one for the pristine OC_1C_{10}PPV substrate and one for the K/OC_1C_{10}PPV system. In these spectra each compositional element is identified as a step in the TOF signal and can be traced until the next element (with lower mass number) appears. The step due to the presence of K is clearly visible in the uppermost spectrum. The photon peak shown in the spectrum is produced by inelastic processes that involve outer shell electrons from incident and target particles[34] and is employed for time calibration. The NICISS signal starting at 3 μs increases as a result of hydrogen recoils that contribute to the spectrum in both ionized and neutral form. Their presence in the spectrum remains over the complete time scale.[31]

In order to obtain the depth profiles for K, the NICISS signal of pristine PPV is subtracted from the reference OC_1C_{10}PPV/K spectrum. The depth scale for K is derived from the time of flight scale taking into account the stopping power of the projectiles in the hydrocarbons.[30] The inelastic loss of energy during backscattering of K was assumed to be 10 eV. Since it was not measured during the experiments the leading mark of the depth scale can be determined only with an accuracy of ±2 Å. The K concentration is determined by

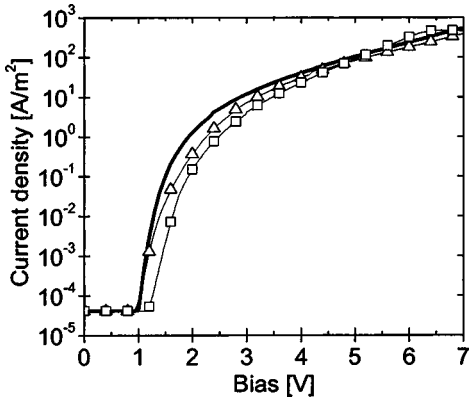

FIG. 2. $I-V$ characteristics on Al/K/OC_1C_{10}PPV/ITO LED structures with varying deposition coverage: 3.9×10^{12} (triangles) and 1.2×10^{14} (squares) atoms/cm^2 and without K (thick solid curve). At a coverage of 3.4×10^{13} atoms/cm^2 or more the current onset remains at 1.45 V.

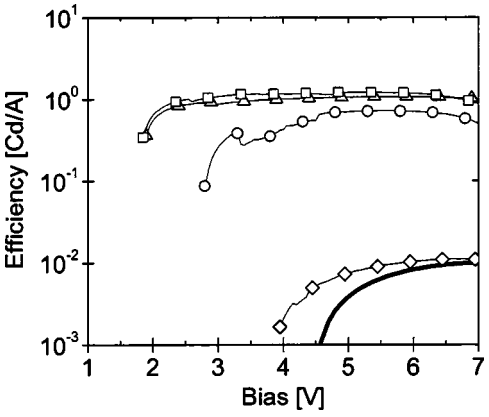

FIG. 4. Efficiency of Al/K/OC_1C_{10}PPV/ITO LED structures with varying deposition coverage: 3.9×10^{12} (diamonds), 2.0×10^{13} (circles), 3.4×10^{13} (triangles), and 1.0×10^{14} K (squares) atoms/cm^2 and without K (thick solid curve).

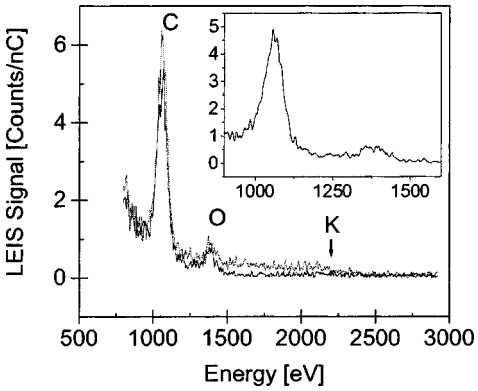

FIG. 5. LEIS spectra obtained from $K/OC_1C_{10}PPV/ITO$ stacking structures. Two spectra are shown with different quantities of deposited K atoms/cm^2 (black: 0.71×10^{14}; gray: 1.2×10^{14}) and one with pristine $OC_1C_{10}PPV$ (inset).

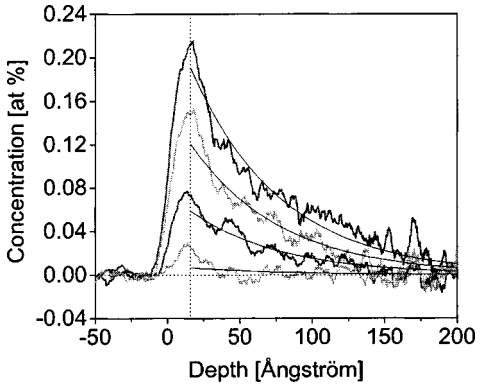

FIG. 7. K diffusion profiles determined by NICISS (smoothed over ten data points). The total deposition is calculated by integration of the spectra and amounts (from top to bottom) to 1.2×10^{14}, 7.1×10^{13}, 3.5×10^{13}, and 3.9×10^{12} atoms/cm^2. The time between manufacturing and conducting the ion scattering measurements is 2, 18, 18, and 6 days, respectively. The solid curves through the spectra are fits to an exponential decay function with a characteristic decay length of 62 Å.

relating the count rate to the C signal including corrections for the C atomic fraction ($\Phi_C=39\%$) and the differential cross sections.

Figure 7 shows the concentration-depth profiles for $K/OC_1C_{10}PPV$ structures with increasing amounts of K deposition. The profiles show that the K concentration increases from negligible at the surface to a maximum at a depth of 16 Å. For depths larger than 16 Å the K concentration decreases. The profiles are not significantly influenced by the depth resolution: deconvoluted depth profiles as calculated using an an algorithmic deconvolution procedure for a Gaussian distribution function with full width half maximum of 9.3 Å for K, are nearly identical to the measured data. Comparing the concentration profiles together with the time difference between manufacturing and analyzing the substrates (see caption Fig. 7) it is evident that the diffusion profiles are irrespective of time. Thus at the moment we conduct the ion scattering investigations the K concentrations are metastable and diffusion has stopped. Therefore, we must include a trapping mechanism in order to describe the diffusion.

The diffusion process was thus modeled by assuming Fickian diffusion in a semi-infinite plane from an instantaneous source with an irreversible first order ''trapping'' reaction[35]

$$\partial C/\partial t = D\partial^2 C/\partial x^2 - kC, \tag{1}$$

which equals zero in case we consider the steady state situation. We assume this diffusion to begin at the observed maximum (16 Å below the surface). Here k and D are the trapping and chemical diffusion constant, respectively, and $C(x)$ the K concentration as a function of depth x. The solution to this differential equation is

$$C(x) = Mq\exp(-qx) \quad \text{for} \quad (x>0), \tag{2}$$

where M is the total amount of diffusing substance and $q=(k/D)^{1/2}$. From the resulting fits shown in Fig. 7 the characteristic decay length, $1/q$, is determined to be independent of K concentration and amounts to 62 Å.

In short, we note that in $K/OC_1C_{10}PPV$ systems both subsurface and bulk diffusion are substantial. Moreover, in comparison with the emissive layer of 1000 Å, the 200 Å at which K is detected, is significant. The depth profile is approximated by an exponential decaying concentration with its maximum below the polymer surface at ~16 Å.

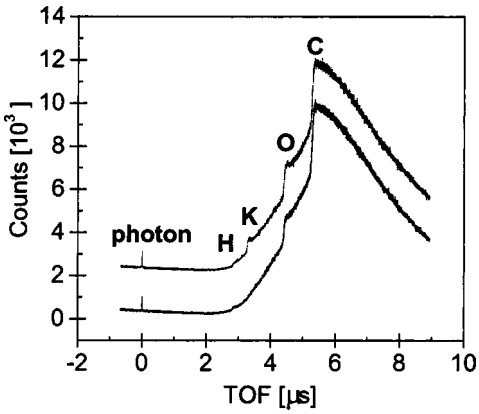

FIG. 6. NICISS on an $OC_1C_{10}PPV/ITO$ stacking structure with K deposition (upper) and without (lower). For clarity the upper spectrum is raised by 2000 counts.

IV. DISCUSSION

A. Diffusion profile

In the following section we differentiate between two diffusion processes, which we refer to as subsurface diffusion and bulk diffusion. In order to minimize the free energy the main contribution stems from the surface energy: the component with highest surface energy will diffuse into the other component until it is completely screened from the vacuum and the surface energy is minimized: we will refer to this as subsurface diffusion. A minor contribution to the free energy originates from the increase in entropy by lowering the concentration gradient in the system, which results in bulk diffusion. In addition, the free energy is also lowered by the decrease in chemical potential through charge transfer between the components.

The driving force for subsurface diffusion is the difference in surface energy between the metal particles, γ_M, on one side and the polymer surface energy, γ_P, and the interfacial energy, γ_{MP}, on the other. Subsurface diffusion occurs in case the inequality $\gamma_M > \gamma_P + \gamma_{MP}$ holds. In general the surface energy for polymers is much lower than that for metals ($\gamma_P \approx 10^{-2}$ J m^{-2} and $\gamma_M \approx 10^{-1}-10^{0}$ J m^{-2}). An estimate for the interfacial energy for a range of polymer/inorganic material combinations is given for instance by Fowkes[36] and the inequality holds for most systems. In general, kinetics, determined by substrate temperature and deposition rate, may prevent diffusion in the polymer leading to aggregation.[37]

The K depth profiles shown in Fig. 7 clearly indicate that the subsurface concentration is higher than the surface concentration. The LEIS spectrum even demonstrates the complete absence of K at the outermost surface layer within the detection limit of 100 ppm and therefore subsurface diffusion has been established. Whether the atoms at the surface diffuse by available vacancies within the polymer matrix or whether they are immediately covered by alkoxy side groups in order to lower the surface energy cannot be deduced from these experiments. It should be noted that the maximum K concentration does not occur just below the surface, but somewhat deeper (16 Å). As soon as the K is situated more than roughly 4 Å below the surface, the surface free energy has already been significantly reduced. The observation that the maximum K concentration occurs deeper than this, indicates that the position of this maximum must result from the details of the diffusion and trapping mechanisms.

Bulk diffusion of K extends over a range of 200 Å and detection beyond this depth is limited by our experimental method. As the diffusion profiles do not seem to be affected by time, we assume a stationary K distribution, from which the importance of trapping then immediately can be concluded. In absence of trapping the depth profiles should have converged to a spatially homogeneous distribution over time, which we do not observe.

UPS measurements have clearly shown that charge transfer occurs between the K and the conjugated backbone of the polymer, resulting in doping induced gap states.[4] The maximum doping level occurred at one K atom per monomer repeating unit, which assures that complete charge transfer occurs in the samples studied here. This charge transfer will also have an immediate affect on diffusion: since cations repel each other their diffusion is not impeded by the formation of immobile clusters and in addition, as bulk diffusion is generally considered to proceed through the mechanism of vacancy hopping, the smaller ion size compared to their neutral form promotes diffusion as well.[38]

The repulsive Coulomb interaction between cations does not significantly affect the observed depth profiles, as electrons donated to the π-conjugated system will attempt to screen these positive sites and freely rotating dipoles are formed. The average potential energy decays as $1/r^6$ and compared to the kinetic energy term of $3/2\ kT$, becomes negligible at length scales in the order of Angströms. Here r is the distance between two dipoles, k is the Boltzmann constant, and T the temperature ($=293$ K). An explanation for trapping may be found in the density of defects which limits the conjugation length. The electrons will be localized to typically 6–10 monomer units and due to electrostatic forces the ion diffusion is restricted. The length of such a conjugated segment (estimated at 50 Å using the length of 6.3 Å for one monomer unit) and their random orientation with respect to the surface, is in reasonable agreement with the characteristic length of 62 Å for the decaying exponential we obtained for fitting. This of course only holds when charge transfer results on a time scale much smaller than diffusion.

B. Electroluminescence

Here the effect of chemical (charge transfer) doping leading to the enhanced performance is discussed in terms of the electronic transport.

Generally, the built-in potential is approximated by the difference in work function of anode and cathode,[39] assuming vacuum level alignment at the metal–polymer interfaces.[40] However, the overall absence of K at the surface (Fig. 5) rules out the explanation of matching the lowest unoccupied molecular orbital (LUMO) of OC_1C_{10}PPV to the work function of a metallic K layer. This is confirmed by UPS studies:[2,3] a decreasing work function due to alkali deposition is exclusively measured at alkali densities much higher than used here (10 and 40 at. % for Rb[3] and Na[2], respectively). The formation of (bi)polaron states leads to a shift of the Fermi energy level to lower binding energy close to the polymer surface.[3] The Fermi level of Al will be able to align to this Fermi energy level and consequently we ascribe the increase in built-in potential of 250 mV to a transition from vacuum level to Fermi level alignment as has been observed before by Greczynski *et al.*.[41]

The enhanced luminescence could partly be explained by the increased built-in potential, for the alignment of the Al work function to the increased polymer Fermi energy level will lower the barrier for electron injection. However, this cannot explain the concentration dependent luminescence upon further deposition as the current onset remains unaffected.

It was experimentally determined that as a consequence of difference in carrier mobility in PPVs, current–voltage ($I-V$) characteristics for double injection structures are dominated by the hole current density.[14] Therefore, electron–hole recombination occurs close to the polymer/cathode interface as was shown by model calculations for a pLED with either ohmic or tunneling contacts.[42,43] In addition nonradiative energy transfer for emitting dipoles as a function of distance from a metallic mirror has been experimentally demonstrated and its impact on the radiative recombination efficiency for MEH–PPV ranged up to 60 nm from the Al cathode.[11] Accordingly we attribute our increase in EL (efficiency) with increasing K deposition to a shift of the recombination zone away from the cathode.

Chemical doping of the polymer surface layer by K deposition may lead to three physical mechanisms, each of which is able to account for this shift: (1) an enhanced electron injection; (2) an increase in electron mobility due to the newly formed electronic states close at the LUMO; and (3)

the presence of donor electrons that are available for recombination in the polymer layer through doping (through the formation of recombination centers).

The first two mechanisms can potentially be observed by electrical characterization. However, the analytical solution to the problem of double injection into an insulator in steady state[44] shows that the hole current prevalence over the total current remains even for an increase of electron current by 2 orders of magnitude.[45] Thus in order to demonstrate the validity of either of these two possibilities one should attempt to reduce the hole current by increasing its injection barrier or, better, by manufacturing an electron only device.

For the luminescence properties the exact concentration-depth profile will be important and should be taken into account in case the second and third mechanism apply: in general the bandwidth of the density of states introduced by doping is concentration dependent and should be reflected in the electron mobility. Also, the position of the donated electrons, where excitons may be formed, will closely correspond to that of the K cations in the interfacial region and hence may dictate the non-radiative energy transfer to the Al mirror. The data presented here do not allow for any discrimination between these mechanisms and further qualification of the electronic transport is thus omitted.

The above mentioned mechanisms responsible for the increase in EL are based on the occurrence of charge transfer and subsequently the formation of gap states. At first glance this is in contradiction with former reports where in fact these gap states were assigned to quench the PL in PPV derivatives.[9] Moreover it was demonstrated that by removing these states by oxidation the PL[9] property could recover. However, since it is known that Al neither diffuses[46] nor introduces these gap states[4] and merely opens a nonradiative decay channel,[11] we propose that for the EL a shift of the recombination zone away from the Al cathode is dominant over the exciton quenching mechanism by the formation of gap states at submonolayer deposition.

Cao *et al.*[16] discussed the relation between device performance and the extension of the alkali doping region: they speculated that the diffusion rate is a much more important factor than the alkali work function during degradation. Our results confirm this, since we observe that even submonolayers at room temperature result in a diffusion region of about 200 Å. Cao *et al.* did not observe such concentration dependent behavior as reported here, but demonstrated that due to alkali deposition beyond 100 Å the PL efficiency severely decreased, which they attributed to quenching. We did not observe a decrease in EL efficiency, however it should be pointed out that our K coverage was far below this 100 Å.

V. SUMMARY AND CONCLUSION

The introduction of K onto poly(dialkoxy-p-phenylene vinylene) (OC_1C_{10}PPV) by physical vapor deposition has been applied in polymer LEDs, using ITO and Al as the anode and cathode, respectively. The stacking structures were characterized by LEIS, NICISS, and EL in order to study the interface of the alkali/PPV system in relation to its performance.

The complete absence of K at the polymer surface and bulk diffusion up to 200 Å at a K concentration of 1.2×10^{14} atoms cm^{-2} was established by ion scattering analysis. Depth profiles have been extracted from the NICISS spectra, and bulk diffusion was modeled by introducing a trapping parameter. We determined a characteristic decay length of 62 Å, and we speculate that the confined conjugation length is the source for trapping and determines the decay length.

EL measurements clearly demonstrate a concentration dependent behavior: with increasing deposition an enhancement in luminescence and efficiency was observed (more than 2 orders in magnitude). The observed increase in built-in potential can at most partially account for this effect. We propose that the deposition of K actually results in a shift of the recombination zone, which can be either due to an improved charge balance or the presence of recombination centers in the interfacial layer. This will be pursued in further investigations.

In contrast to the common assumption in modeling charge carrier dynamics in *p*LEDs, this study clearly indicates that physical vapor deposition of alkali metals (and presumably earth alkaline metals as well) onto soft condensed systems cannot generally be depicted as simple layered stacking structures. Moreover, we demonstrate that the formation of gap states in the polymer layer results in an increased EL for deposition coverage up to 1.2×10^{14} atoms/cm^2 and that the gap state induced quenching mechanism as was pointed out by Park *et al.*,[9] is of secondary importance compared to the nonradiative decay by energy transfer to the Al mirror.

ACKNOWLEDGMENTS

The authors gratefully thank Professor H. Morgner for providing access to the NICISS setup. This research was supported by grants from the Dutch Foundation for Material Research (FOM).

[1] J. H. Burroughes, D. D. C. Bradley, A. R. Brown, R. N. Marks, K. Mackay, R. H. Friend, P. L. Burn, and A. B. Holmes, Nature (London) **347**, 539 (1990).
[2] M. Fahlman, D. Beljonne, M. Lögdlund, R. H. Friend, A. B. Holmes, J. L. Brédas, and W. R. Salaneck, Chem. Phys. Lett. **214**, 327 (1993).
[3] G. Iucci, K. Xing, M. Lögdlund, M. Fahlman, and W. R. Salaneck, Chem. Phys. Lett. **244**, 139 (1995).
[4] J. Birgerson, M. Fahlman, P. Bröms, and W. R. Salaneck, Synth. Met. **80**, 125 (1996).
[5] G. Greczynski, M. Fahlman, and W. R. Salaneck, Appl. Surf. Sci. **166**, 380 (2000).
[6] H. Ishii, K. Sugiyama, E. Ito, and K. Seki, Adv. Mater. (Weinheim, Ger.) **11**, 605 (1999).
[7] I. G. Hill, A. Rajagopal, A. Kahn, and Y. Hu, Appl. Phys. Lett. **73**, 662 (1998).
[8] J. Yoon, J. J. Kim, T. W. Lee, and O. O. Park, Appl. Phys. Lett. **76**, 2152 (2000).
[9] Y. Park, V.-E. Choong, B. R. Hsieh, C. W. Tang, and Y. Gao, Phys. Rev. Lett. **78**, 3955 (1997).
[10] Y. Park, V. Choong, E. Ettedgui, Y. Gao, B. R. Hsieh, T. Wehrmeister, and K. Müllen, Appl. Phys. Lett. **69**, 1080 (1996).
[11] H. Becker, S. E. Burns, and R. H. Friend, Phys. Rev. B **56**, 1893 (1997).
[12] G. G. Andersson, H. H. P. Gommans, A. W. Denier van der Gon, and H. H. Brongersma, J. Appl. Phys. **93**, 3299 (2003).
[13] P. S. Davids, I. H. Campbell, and D. L. Smith, J. Appl. Phys. **82**, 6319 (1997).

[14] P. W. M. Blom and M. J. M. de Jong, IEEE J. Sel. Top. Quantum Electron. **4**, 105 (1998).
[15] F. Faupel, Mater. Res. Soc. Symp. Proc. **511**, 15 (1998).
[16] Y. Cao, G. Yu, I. D. Parker, and A. J. Heeger, J. Appl. Phys. **88**, 3618 (2000).
[17] H. M. Lee, K. H. Choi, D. H. Hwang, L. M. Do, T. Zyung, J. W. Lee, and J. K. Park, Appl. Phys. Lett. **72**, 2382 (1998).
[18] Y. E. Kim, H. Park, and J. J. Kim, Appl. Phys. Lett. **69**, 599 (1996).
[19] J. Yoon, J. J. Kim, T. W. Lee, and O. O. Park, Appl. Phys. Lett. **76**, 2152 (2000).
[20] P. Piromreun, H. S. Oh, Y. Shen, G. G. Malliaras, J. C. Scott, and P. J. Brock, Appl. Phys. Lett. **77**, 2403 (2000).
[21] T. M. Brown, R. H. Friend, I. S. Millard, D. J. Lacey, J. H. Burroughes, and F. Cacialli, Appl. Phys. Lett. **79**, 174 (2001).
[22] S. Li, E. T. Kang, K. G. Neoh, Z. H. Ma, K. L. Tan, and W. Huang, Appl. Surf. Sci. **181**, 201 (2001).
[23] J. Birgerson, F. J. J. Janssen, A. W. Denier van der Gon, Y. Tsukahara, K. Kaeriyama, and W. R. Salaneck, Synth. Met. **132**, 57 (2002).
[24] D. Braun, E. G. J. Staring, R. C. J. E. Demandt, G. L. J. Rikken, Y. A. RR. Kessener, and A. H. J. Venhuizen, Synth. Met. **66**, 75 (1994).
[25] G. G. Andersson, M. P. de Jong, F. J. J. Jansen, J. M. Sturm, L. J. van IJzendoorn, A. W. Denier van der Gon, M. J. A. de Voigt, and H. H. Brongersma, J. Appl. Phys. **90**, 1376 (2001).
[26] H. H. Brongersma and P. M. Mul, Chem. Phys. Lett. **14**, 380 (1973).
[27] G. J. A. Hellings, H. Ottevanger, S. W. Boelens, C. L. C. M. Knibbeler, and H. H. Brongersma, Surf. Sci. **162**, 913 (1985).
[28] H. Niehus and G. Comsa, Nucl. Instrum. Methods Phys. Res. B **15**, 122 (1986).
[29] G. Andersson and H. Morgner, Surf. Sci. **405**, 138 (1998).
[30] G. Andersson and H. Morgner, Nucl. Instrum. Methods Phys. Res. B **155**, 357 (1999).
[31] G. Andersson and H. Morgner, Surf. Sci. **405**, 138 (1998).
[32] G. Marletta, Nucl. Instrum. Methods Phys. Res. B **46**, 295 (1990).
[33] P. Bertrand and Y. De Puydt, Nucl. Instrum. Methods Phys. Res. B **78**, 181 (1993).
[34] White, *Inelastic Ion-Surface Collisions* (Academic, New York, 1977).
[35] J. Crank, *The Mathematics of Diffusion*, 2nd ed. (Oxford University Press, Bristol, 1975), p. 329.
[36] F. M. Fowkes, Ind. Eng. Chem. **56**, 40 (1964).
[37] G. J. Kovacs and P. S. Vincett, J. Colloid Interface Sci. **90**, 335 (1982).
[38] F. Faupel, Mater. Res. Soc. Symp. Proc. **511**, 15 (1998).
[39] G. G. Malliaras, J. R. Salem, P. J. Brock, and C. Scott, Phys. Rev. B **58**, R13411 (1998).
[40] H. Ishii, K. Sugiyama, E. Ito, and K. Seki, Adv. Mater. (Weinheim, Ger.) **11**, 605 (1999).
[41] G. Greczynski, Th. Kugler, and W. R. Salaneck, J. Appl. Phys. **88**, 7187 (2000).
[42] P. W. M. Blom, M. C. J. M. Vissenberg, J. N. Huiberts, H. C. F. Martens, and H. F. M. Schoo, Appl. Phys. Lett. **77**, 2057 (2000).
[43] G. G. Malliaras and J. C. Scott, J. Appl. Phys. **83**, 5399 (1998).
[44] R. H. Parmenter and W. Ruppel, J. Appl. Phys. **30**, 1548 (1959).
[45] Applying the measured mobilities for both holes and electrons at OC_1C_{10} PPV as a function of bias from 13.
[46] M. Atreya, S. Li, E. T. Kang, K. G. Nech, Z. H. Ma, and K. L. Tan, J. Vac. Sci. Technol. A **17**, 853 (1999).